

Layered Silicate Nanocomposites Based on Various High-Functionality Epoxy Resins: The Influence of Cure Temperature on Morphology, Mechanical Properties, and Free Volume

Ole Becker,[†] Yi-Bing Cheng,[†] Russell J. Varley,[‡] and George P. Simon^{*,†}

School of Physics & Materials Engineering, Monash University, Clayton, Victoria 3800, Australia, and CSIRO Molecular Science, Clayton, Victoria 3169, Australia

Received August 19, 2002

ABSTRACT: This paper investigates the relationship between cure temperature, morphology, and mechanical properties of di-, tri-, and tetrafunctional high-performance, epoxy layered-silicate nanocomposites. Wide-angle X-ray analysis (XRD) was carried out at different stages of cure to monitor organoclay exfoliation kinetics. It was found that some (small) degree of conversion was required to obtain significant intercalation. The nanocomposite morphology was also probed using transmission electron microscopy, XRD, and positron annihilation lifetime spectroscopy. The bifunctional DGEBA resin gave better exfoliation than the resins of higher functionalities. This is attributed to better catalysis of the intragallery reaction by the organo-ions which reside within the galleries. Higher cure temperatures were also found to improve clay delamination and simultaneously increased toughness and modulus in case of the DGEBA- and TGAP-based materials. Free volume properties did not vary significantly between resins or with cure temperature and generally followed the rule of mixtures, although there was a suggestion that the presence of clay leads to increased free volume. This was consistent with decreased glass transition temperatures upon addition of layered silicate, ascribed to disruption, and decreased cross-link density in interfacial regions of clay and epoxy matrix.

Introduction

A recent approach to improve and diversify the properties of polymeric materials has been through the incorporation of layered silicates into the polymer matrix. Being only 1 nm thick with an aspect ratio of up to 1000, these mica-like fillers have shown significant improvement in materials performance at relatively low concentrations, in comparison to much higher levels of commonly used fillers. There are a number of potential improvements due to inclusion of layered silicates in polymers: increased modulus and toughness, improved barrier properties and flame retardance, as well as better dimensional and thermal stability. The development of this relatively new group of nanocomposite material has recently been summarized by various authors.^{1–4}

The basic principle behind the formation of layered silicate epoxy nanocomposites is that both the resin and hardener molecules are able to intercalate into, and react within the silicate interlayer galleries. The nanocomposite structures present after cure can be broadly divided into two types: intercalated nanocomposites, in which the silicate is well-dispersed in a polymer matrix with polymer chains inserted into silicate layers that retain their lateral order, and exfoliated nanocomposites where the silicate platelets become fully separated or delaminated, essentially individually dispersed in the polymer matrix. However, these terms describe only ideal cases, and it is more likely that the description of a real morphology falls somewhere between these extremes.^{5,6}

The mechanism proposed for the formation of such epoxy nanocomposites is that the penetrating monomers

swell the silicate layers until a thermodynamic equilibrium is reached between the polar resin, curing agent blend, and the high surface energy of the silicate layers.^{7,8} Decreasing polarity during reaction of the resin in the galleries displaces the equilibrium, causing more monomers to diffuse into, and react within, the silicate galleries. Depending on the layered silicate charge density,^{7,8} the nature of the interlayer exchanged ion,^{9–11} the cure conditions,^{12–14} the curing agent,^{12,15} and the resin (as is reported in this work), the resultant epoxy nanocomposite will show either an intercalated or exfoliated morphology. Recently, Chin et al.¹⁶ have shown for a *m*-phenylenediamine (MPDA)/DGEBA/octadecylamine-layered silicate system that the resin/curing agent ratio can also influence the exfoliation process. In their work it was found that under-stoichiometric amounts of MPDA gave better exfoliation than stoichiometrically balanced systems. It was assumed that the lower concentration of curing agent reduced the role of the extragallery cross-linking reaction more than it did the slower diffusion-controlled reaction within the gallery. Kornmann et al.¹² have investigated the effect of three different curing agents (poly(propylene glycol) bis(2-aminopropyl ether), 3,3'-dimethylmethylethylene di-(cyclohexylamine), and bis(*p*-aminocyclohexylamine) upon the organoclay exfoliation in a DGEBA-based system. In their work it was found that exfoliation of the organoclay occurred for the cycloaliphatic diamine-cured DGEBA nanocomposite only at higher temperatures. Key issues found to encourage exfoliation were thought to be reactivity and diffusion rates (mobility and flexibility) of the curing agent due to their effect on extragallery and intragallery reaction rate. While in some cases improved exfoliation has been reported for increased cure temperatures,^{9,12–14,17} other systems were found not to be affected within a certain temperature range.^{17,18}

[†] Monash University.

[‡] CSIRO Molecular Science.

* To whom correspondence should be addressed: Fax + 61 (0)3 9905 4940; e-mail george.simon@spme.monash.edu.au.

Table 1. Different Cure Profiles of Epoxy Nanocomposites Synthesis

sample identification (°C)	step 1	step 2	step 3	step 4
80	80 °C for 12 h	130 °C for 1 h	160 °C for 12 h	200 °C for 2 h
100	100 °C for 2 h	130 °C for 1 h	160 °C for 12 h	200 °C for 2 h
120	120 °C for 2 h	130 °C for 1 h	160 °C for 12 h	200 °C for 2 h
140	140 °C for 2 h		160 °C for 12 h	200 °C for 2 h
160			160 °C for 12 h	200 °C for 2 h

In the field of thermosetting nanocomposites, the vast majority of work reported to date has been on more flexible resins systems with moderate glass transition temperatures, generally using the bifunctional diglycidyl ether of bisphenol A (DGEBA) resin. However, most of the aerospace and other high-performance applications require resin systems of improved mechanical properties and higher glass transition temperatures such as trifunctional triglycidyl *p*-aminophenol (TGAP) and tetrafunctional tetraglycidyl diaminodiphenylmethane (TGDDM)-based resins. Very recent reports on high-performance epoxy nanocomposites have shown some promising results,^{5,17} but little work has been reported in this area. The following investigation is focused on how the kinetics of intercalation, morphology, and mechanical properties of high-performance, high-functionality epoxy nanocomposites can be optimized by manipulating cure conditions and resin type. In addition, the first report on free volume in epoxy nanocomposite systems using positron annihilation lifetime spectroscopy (PALS) is presented to give an insight into the molecular structure of the nanocomposite, as a function of reaction conditions.

Experimental Section

The three different epoxy resins used in this work were diglycidyl ether of bisphenol A (DGEBA), DER 331 Dow epoxy resin, triglycidyl *p*-aminophenol (TGAP), Araldite MY 510 of Ciba Specialty Chemicals, and tetraglycidyl diaminodiphenylmethane (TGDDM), Araldite MY 720, of Ciba Specialty Chemicals. The hardener, Ethacure 100, of Albemarle Corp. is a mixture of two diethyltoluenediamine (DETDA) isomers (74–80% 2,4-isomer and 18–24% 2,6-isomer). Resins were mixed with 2.5, 5, or 7.5 wt %, respectively, of an octadecylammonium ion modified montmorillonite, Nanomer I.30E, from Nanocor Inc. for 45 min at 75 °C. After addition of the hardener, the blend was degassed under vacuum for 45 min at 60 °C. The blends were poured into PTFE-coated molds and cured using different temperature profiles. The various cure cycles are given in Table 1 and are labeled by their initial cure temperature. Samples for following exfoliation as a function of cure studies and differential scanning calorimetry (DSC) measurements were produced using the same procedure as above. The reactive mixtures were poured into aluminum trays and cured for different periods of time at 140 °C.

Wide-angle X-ray diffraction (XRD) analysis of the fully cured systems was performed using a Rigaku Geigerflex generator with a wide-angle goniometer. An acceleration voltage of 40 kV and current of 22.5 mA were applied using Ni-filtered Cu K α radiation. Measurements were taken in a range of $2\theta = 1^\circ$ – 22° . XRD measurements of partially cured (in some cases liquid) systems were obtained with a Siemens D500 diffractometer with a back monochromator and a Cu cathode in a range of $2\theta = 1^\circ$ – 10° .

DSC analyses were carried out on a Perkin-Elmer DSC-7 using Pyris software. Prior to measurement, calibration was performed using indium and zinc standards. Samples of 5–8 mg were sealed in aluminum pans and heated from 50 to 350 °C at a scanning rate of 10 °C/min.

Transmission electron microscope samples were cut using a Porter-Blum MT-2B ultramicrotome with a DiaTech (Knoxville) diamond knife. Cuts were made at an angle of 6° and a

cutting velocity of about 0.1 mm/s. Samples were collected on hexagonal 300 mesh copper grids. Micrographs were than obtained from a Philips CM20 transmission electron microscope operating at 200 kV in bright field mode.

FTIR analysis was performed on a Perkin-Elmer Spectrum GX FT-IR system. Samples of 1.5 mm thickness were scanned in a wavenumber range of 8000–4000 cm^{-1} .

Positron annihilation lifetime spectroscopy (PALS) was applied to determine free volume properties of the cured nanocomposites. A detailed background on the theory and technique of PALS can be found elsewhere.^{19–21} Briefly, the antiparticle of an electron, the positron, is used to investigate the free volume between polymer chains. The “birth” of the positron can be detected by the release of a γ -ray of characteristic energy, which occurs approximately 3 ps after positron emission when the ^{22}Na decays to ^{22}Ne . Once inside the polymer material, the positron forms one of two possible types of positroniums, an orthopositronium or a parapositronium, obtained by pairing with an electron abstracted from the polymer environment. The decay spectra are obtained by the “death” event of the positron, parapositron, or orthopositron species. By appropriate curve fitting, the lifetimes of the various species and their intensity can be determined. The lifetime of orthopositronium (τ_3) and intensity (I_3) have been found to be indicative of the free volume in the polymer system since this is where the relevant species become localized and form. τ_3 is related to the size of the free volume sites and I_3 to their number concentration. Since τ_3 is related to the radius, $\tau_3^3 I_3$ is used in this work as an indication of total free volume fraction.

The PALS unit used was an automated EG&G Ortec fast–fast coincidence system with a ^{22}Na radioactive source and a resolution of 270 ps measured on ^{60}Co . A 1 mm diameter spot source of ^{22}Na was obtained from dropping a $^{22}\text{NaCl}$ solution onto very thin titanium foils, with a resultant activity of 40 μCi . Experiments were run in a thermally stable environment at 22 °C. No source correction was required, confirmed by testing of highly annealed and polished aluminum, which results in the well-known, single decay process. Each spectrum consists of 30 000 peak counts and the data were fitted using the PFPOSFIT program.²²

Results and Discussion

The influence of the cure temperature on the morphology of the different epoxy nanocomposite systems was investigated. A range of DETDA-cured epoxy nanocomposites based on the three different resins (DGEBA, TGAP, and TGDDM) containing 7.5% organoclay were prepared at different initial cure temperatures (Table 1). The distance between two silicate layers, the *d*-spacing, was determined following cure using wide-angle XRD. An example for the XRD traces as a function of the initial cure temperature is illustrated in Figure 1 for the series of TGDDM-based nanocomposites. Identifications of the (001) and (002) diffraction peaks are summarized for all investigated systems in Table 2. The (00 l) peaks represent the reflections due to the stacks of the clay layers. The shift of those peaks in the XRD spectrum thus reflects changes in distance between the silicate platelets. The initial *d*-spacing of the dried organoclay was determined to be 23 Å. In each nanocomposite system a peak can be found at $2\theta =$

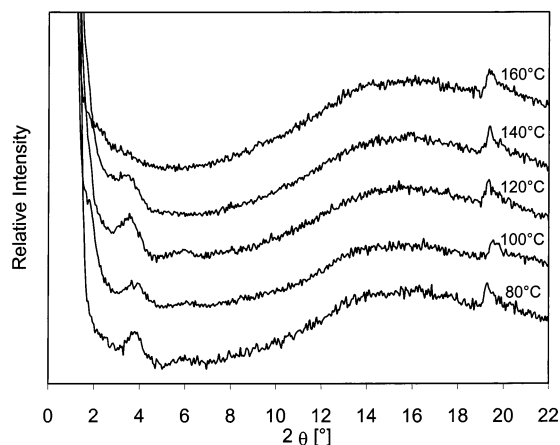


Figure 1. WAXS of DETDA-cured TGDDM nanocomposites containing 7.5% organoclay, cured at different temperature profiles.

Table 2. (001) and (002) Diffraction Peaks of the Silicates and Correlating *d*-Spacing in the DETDA-Cured Nanocomposites Containing 7.5% Organoclay As Determined from WAXS Measurements

resin system	cure temp [°C]	(001) plane peak	(002) plane peak	<i>d</i> -spacing of (001) plane [Å]	<i>d</i> -spacing [Å] (TEM)
TGAP	80	42.0	20.5	42 ± 2	^a
TGAP	100	no peak	25.0	50 ± 2	46
TGAP	120	46.5	22.8	46 ± 2	^a
TGAP	140	49.0	22.9	47 ± 2	^a
TGAP	160	no peak	26.0	52 ± 2	50
TGDDM	80	no peak	22.6	45 ± 2	^a
TGDDM	100	no peak	22.9	46 ± 2	45
TGDDM	120	no peak	24.2	48 ± 2	^a
TGDDM	140	no peak	24.9	50 ± 2	^a
TGDDM	160	no peak	no peak	exfoliated	60
DGEBA	100	no peak	no peak	exfoliated	85
DGEBA	160	no peak	no peak	exfoliated	95

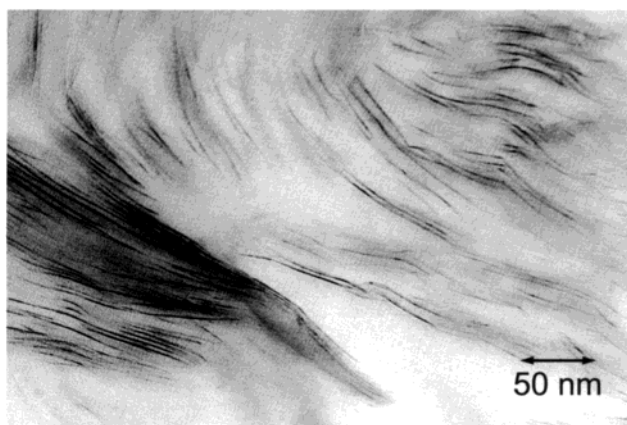
^a Not determined.

approximately 19.5°. This peak represents the (110) reflection of the montmorillonite.²³ The (*hk*0) plane characterizes the atomic arrangement in the plane that is parallel to the *z*-axis. This peak is therefore independent of the distance between silicate platelets, and its location can be used as a reference.

XRD traces of the DGEBA based systems did not show any peaks in the low-angle range, indicating that any cure temperature between 80 and 160 °C leads to a well-intercalated or exfoliated nanocomposite structure. It should be noted that the lowest angle able to be measured here was $2\theta = 1^\circ$, which correlates with a *d*-spacing of 88 Å. In addition, the large increase in intensity of the XRD signal toward lower angles may overlap or interfere with peaks in that region and therefore obscure signals related to a *d*-spacing above 50 Å. This may occur particularly if the platelets show a significant distribution in layer distances, rather than a stronger, sharper peak due to repeat distances of the same length. The traces of the TGAP sample, cured at 80 °C, show a clear (001) peak at $2\theta = 2^\circ$, signifying a *d*-spacing of 45 Å and indicating a high level of intercalation. With increasing cure temperature, the (001) peak in TGAP disappears from the range that can be examined using WAXS, although the (002) peak and a small signal of the (003) peak can be observed. Peaks in the range of 20–25 Å are related to the (002) reflection, representing the half-length of the actual average distance (40–50 Å) between two silicate layers.



(a)

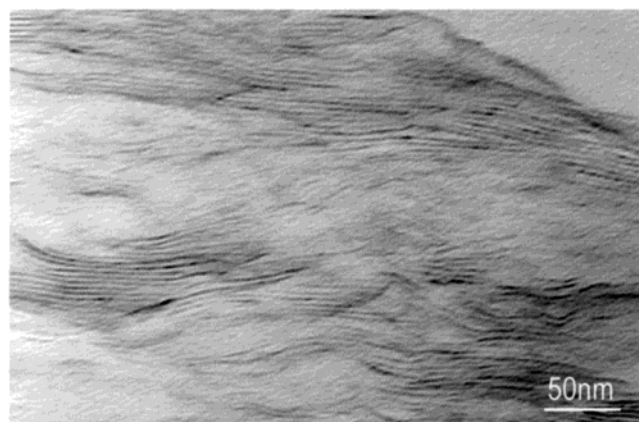


(b)

Figure 2. TEM micrograph of DGEBA nanocomposite cured at 100 °C (a) and 160 °C (b).

The (002) peak itself shifts slightly toward lower angles (higher *d*-spacings) with increasing cure temperature and decreases in intensity. XRD results of the TGAP sample cured at 100 °C seem to show slightly higher values of the *d*-spacing than were expected from the general trend. As shown in Figure 1, the TGDDM-based nanocomposites show a monotonic increase in the average *d*-spacing with increasing cure temperature. No peaks are apparent in the low angle range for the TGDDM-based nanocomposite at a cure temperature of 160 °C. Comparison between the two higher functionality epoxy resin systems shows that, despite its significantly higher viscosity, TGDDM leads to better exfoliation than the less-viscous TGAP system, with both systems showing improved exfoliation at increased cure temperatures.

Because of the range of diffraction angles available from our XRD technique, it is not definitive as to the precise extent that exfoliation in the DGEBA system can be improved with increasing cure temperature. To further investigate the nanocomposite superstructure and to confirm XRD results, transmission electron microscopy (TEM) was performed on each set of nanocomposites cured at 100 and 160 °C, respectively. Micrographs are illustrated in Figure 2 for DGEBA, Figure 3 for TGAP, and Figure 4 for TGDDM nanocomposites containing 7.5% organoclay. The clay platelets in the TGAP and TGDDM nanocomposites cured at 100 °C show a parallel orientation, as commonly reported for most thermoset-layered silicate nanocomposites



(a)



(b)

Figure 3. TEM micrograph of TGAP nanocomposite cured at 100 °C (a) and 160 °C (b).

synthesized via in-situ polymerization.¹⁷ The DGEBA nanocomposites and the high-functionality nanocomposites cured at 160 °C also show this parallel structure with an increased *d*-spacing. However, single platelets and stacks of just a few platelets can also be observed, having been delaminated from the parent tactoids.

The average *d*-spacing of the organoclay was estimated for each system from various measurements of the interlayer distance in different TEM images. The results are summarized in Table 2, together with values determined from the XRD data, both sets being in quite good agreement. TEM images of the DGEBA systems in Figure 2 show a mixture of highly intercalated and partially exfoliated organoclay platelets. Only those platelets that showed a parallel arrangement were considered for measurements of the interlayer distance, determination of the degree of exfoliation being much more difficult. That is, although the ratio of fully exfoliated clay layers compared to highly intercalated parallel oriented platelets has likely changed with cure temperature, this is not readily quantifiable.

For both DGEBA and the high-functionality systems investigated, it was found that increased cure temperature yielded better exfoliation. While this was not the case for a 4,4'-diaminodiphenyl sulfone (DDS)-cured TGDDM nanocomposite,¹⁷ similar results have recently been reported for various DGEBA-based systems.^{12,14} In fact, very recent in-situ small-angle XRD studies by Tolle and Anderson¹⁴ have shown for a *m*-phenylene-diamine-cured DGEBA nanocomposite system using the



(a)

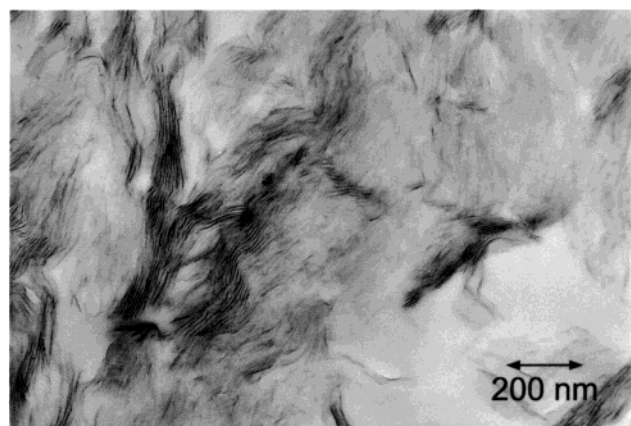


(b)

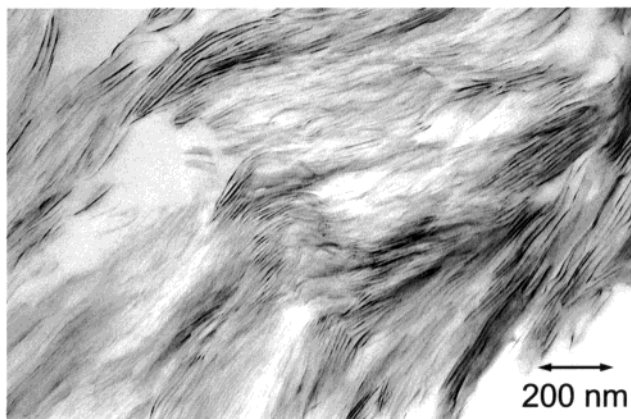
Figure 4. TEM micrograph of TGDDM nanocomposite cured at 100 °C (a) and 160 °C (b).

same commercially available organoclay as in this work, the higher cure temperatures resulted in both earlier initiation of exfoliation and greater silicate spacing. The mechanism of organoclay exfoliation in epoxy-layered silicate nanocomposites has been the focus of various studies,^{7,12,15,24} and it was pointed out that control of intra- and extragallery reaction is the key to overcoming the attractive forces between the silicate layers and achieving exfoliation. The improved organoclay delamination at increased temperatures may be related to a number of aspects, one being that the lower viscosity or enhanced molecular mobility improves mass transfer into the clay galleries. Increased cure temperatures are also known to favor homopolymerization,⁷ and the catalytic effect of the organoclay on both resin-amine cure and homopolymerization²⁵ may shift the equilibrium between inter- and extragallery reaction toward a higher reaction rate within the clay galleries. The structure and chemistry of the epoxy resins are clearly of importance in determining the equilibrium between inter- and extragallery reactions and hence the final morphology of the nanocomposite.

To further understand the influence of the different resin systems on exfoliation of the silicate platelets, the effect of the organoclay on polymerization reaction has been investigated using differential scanning calorimetry (DSC).²⁵ Figure 6 shows DSC traces for the neat resin hardener reaction as well as for the reaction of the organoclay-catalyzed resins (blended with 7.5% organoclay), scanned at 10 °C/min. It can be seen that



(a)



(b)

Figure 5. TEM micrographs of DGEBA nanocomposites cured under shear until close to gelation (a) and the same system without shear forces applied during cure (b).

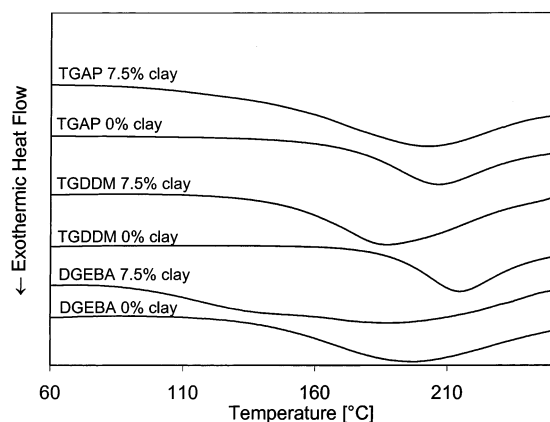


Figure 6. DSC analysis of neat and layered silicate catalyzed cure reaction, determined at a scanning rate of 10 °C/min.

the two resins with the most improvement in d -spacing, DGEBA and TGDDM, show significantly reduced reaction peaks, indicating a strong catalytic effect of the organically modified layered silicate on the cure reactions. The layered silicate containing DGEBA system shows a broad shoulder, or even a second peak, at lower temperatures which is likely to be related to the clay-catalyzed polymerization or homopolymerization. The TGDDM/organoclay/hardener blend also shows a broadened peak with the peak maximum shifted by about 30 °C toward lower temperatures. The TGAP system,

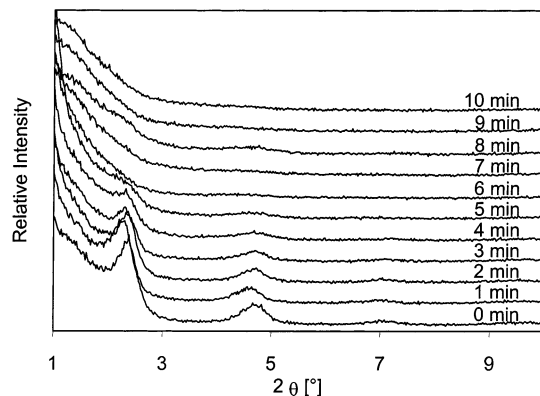


Figure 7. XRD series of the DGEBA-based nanocomposite containing 7.5% organoclay. Traces from the bottom to the top show the development of the interlayer d -spacing during the first 10 min of cure at 140 °C.

which showed least improvement in d -spacing compared to the neat clay, also seems to show the least influence on reactivity, as judged by the temperature location of the DSC cure exotherm peak. To verify the ability of the epoxy resins to move into the organoclay galleries, the zero shear viscosities of the different epoxy resins were determined using parallel plate rheology (at 60 °C). Because of its compact structure, the TGAP resin has shown the lowest zero shear viscosity of 0.04 Pa s, compared with 0.13 for DGEBA and 1.32 for TGDDM. Since the high-viscous TGDDM resin has shown better layer separation than the low-viscous TGAP resin, it becomes clear that at the given reaction temperatures the initial viscosity of the resin is not the determining factor for the exfoliation process. Hence, the ability of the organoclay to act as a catalyst for the different epoxy resins systems, and thus promote the necessary increased reaction rate within the gallery, is necessary to push the clay layers apart. The affinity of the resin toward the clay compatibilizer, which was not investigated in this study, may also be a significant factor in improvement in exfoliation.

To further investigate the formation of the morphology in the DGEBA and TGDDM nanocomposite containing 7.5% organoclay during cure, the relationship between cure time and degree of exfoliation was examined. To follow the silicate layer delamination process during cure, the reactive nanocomposite mixtures were made up as described in the Experimental Section and cured for 1–10 min at 140 °C. After 1 min intervals samples were taken from the cure oven and stored at –20 °C to avoid further reaction. XRD measurements were taken from each sample in a range from $2\theta = 1^\circ$ – 10° . Figure 7 and Figure 8 illustrate the increasing d -spacing of the organoclay for the DETDA-cured DGEBA and TGDDM nanocomposite, respectively, during the first 10 min of cure. In both cases significant changes in the interlayer distance of the clay occurred during the first few minutes. Because of the increasing intensity in the XRD signal at low angles, the (001) peaks are difficult to detect. However, it is observed that this peak soon loses intensity, becoming almost completely absent after 7 min. At the same time, the (002) peak broadens and shifts toward lower angles and thus higher interlayer distances. Because of the resolution of the wide-angle XRD measurement and the fact that exfoliation appears not to be a sudden, but rather a gradual process, it is not possible to say that exfoliation takes place after a precise amount of time; however,

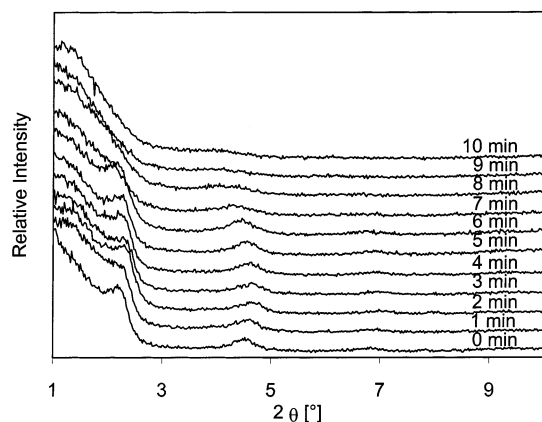


Figure 8. XRD series of the TGDDM-based nanocomposite containing 7.5% organoclay. Traces from the bottom to the top show the development of the *d*-spacing during the first 10 min of cure at 140 °C.

both systems show a high degree of intercalation after 8–10 min. It is interesting to determine the degree of conversion at the stage of cure at which the greater degree of intercalation occurs since this determines the time frame available to mechanically manipulate exfoliation during cure. The residual exothermic enthalpy of reaction of samples at the given cure time was determined using differential scanning calorimetry and compared to the energy of cure of unreacted, catalyzed monomer, allowing the degree of conversion to be determined. The degree of reaction was found to be $22 \pm 3\%$ (8 min) or $26 \pm 3\%$ (10 min) for the DGEBA based system and $13 \pm 3\%$ or $18 \pm 3\%$ (8 and 10 min, respectively) for the TGDDM-based system. In prior work on cure kinetics²⁵ of the same systems, it was demonstrated that the DGEBA-based nanocomposite had a conversion at gelation of about 75% and for the TGDDM some 60%. It is thus clear that major changes in the interlayer distances of these systems occur during the early state of cure, significantly earlier than gelation.

It is well-known that initial mixing (prior to cure) of the organoclay and resin/hardener material leads to only a limited degree of intercalation. This is dependent on the surface energy and polarity of the modified layered silicate and the nature of the resin and hardener. It has been shown that the cure reaction itself may change polarity in the galleries and allow further material to diffuse into the clay galleries and force them apart.⁸ However, TEM images revealed that even in highly intercalated systems that do not show any remnant (001) XRD peaks, the majority of the silicate platelets remained in a parallel, tactoid structure. On the basis of the outcome of the above experiments, it was decided to investigate whether strong stirring forces applied during the early stage of cure when clay platelets are beginning to delaminate could lead to better exfoliation and thus to the formation of a truly exfoliated nanocomposite. DGEBA was mixed with 7.5% organoclay at 140 °C; after 30 min the DETDA hardener was added, with an amine-to-epoxy ratio of 0.9. The blend was further mixed at 500 rpm with a PTFE anchor stirrer while curing. After 10 min the blend was transferred into aluminum trays and further cured at 160 °C for 12 h followed by a postcure of 2 h at 200 °C. TEM images were then taken from microtomed sections of 60 nm thickness and are shown in Figure 5a. For comparison, Figure 5b shows the same system with no shear forces

Table 3. Mechanical Properties of Various DETDA-Cured Epoxy Nanocomposites^a

resin system	organoclay [wt %]	modulus [MPa]	K_{IC} [MNm ^{0.5}]
DGEBA, 100 °C	0	2408 ± 184	0.50 ± 0.05
DGEBA, 100 °C	2.5	2536 ± 91	0.71 ± 0.16
DGEBA, 100 °C	5	2646 ± 166	0.80 ± 0.11
DGEBA, 100 °C	7.5	2883 ± 99	0.86 ± 0.25
DGEBA, 160 °C	0	2871 ± 66	0.91 ± 0.26
DGEBA, 160 °C	2.5	3071 ± 115	1.19 ± 0.24
DGEBA, 160 °C	5	3211 ± 51	1.32 ± 0.17
DGEBA, 160 °C	7.5	3144 ± 41	1.13 ± 0.23
TGAP, 100 °C	0	2758 ± 135	0.49 ± 0.10
TGAP, 100 °C	2.5	2887 ± 209	0.49 ± 0.10
TGAP, 100 °C	5	3120 ± 75	0.63 ± 0.09
TGAP, 100 °C	7.5	3233 ± 84	0.57 ± 0.07
TGAP, 160 °C	0	2863 ± 117	0.52 ± 0.08
TGAP, 160 °C	2.5	3181 ± 270	0.56 ± 0.11
TGAP, 160 °C	5	3516 ± 182	0.65 ± 0.08
TGAP, 160 °C	7.5	3606 ± 78	0.64 ± 0.09
TGDDM, 100 °C	0	3035 ± 38	0.67 ± 0.15
TGDDM, 100 °C	2.5	3225 ± 46	0.90 ± 0.11
TGDDM, 100 °C	5	3349 ± 71	0.98 ± 0.29
TGDDM, 100 °C	7.5	3544 ± 27	1.17 ± 0.04
TGDDM, 160 °C	0	3075 ± 145	0.60 ± 0.21
TGDDM, 160 °C	2.5	3131 ± 53	1.02 ± 0.25
TGDDM, 160 °C	5	3247 ± 67	1.01 ± 0.26
TGDDM, 160 °C	7.5	3540 ± 74	1.19 ± 0.27

^a Values for the 100 °C series are included from our prior work.⁵

applied during cure. The images show that the majority of silicate still remains in tactoids of parallel oriented platelets, with interlayer distances of 80 Å and above. However, it can be seen that some individual platelets are fully separated from their hosting tactoids when such mechanical forces are applied during the exfoliation process. The strategy of improvement of dispersion on a micro- and nanoscale through high shear forces during cure will be the subject of further investigations, including measurements of other properties.

Mechanical Properties. Results for the Young's modulus and fracture toughness of nanocomposite series cured at 100⁵ and 160 °C are summarized in Table 3. All materials show improvement in fracture toughness and modulus compared to the neat material. Within a certain variation there is a monotonic improvement in both properties with increasing organoclay content. Prior work by Zilg et al.²⁶ reported the mechanism of an improved toughness/stiffness balance through the incorporation of organoclay in the epoxy matrix. It was theorized that the exfoliated structure mainly leads to improvement in modulus while the remaining tactoids of intercalated organoclay act as a toughening phase, possibly by the mechanism of energy-absorbing shearing of intercalated clay layers.

The organoclay-containing DGEBA systems cured at 160 °C all show higher values of toughness and stiffness compared to the nanocomposites cured at 100 °C. The TGAP nanocomposites show significant improvement in modulus along with a modest increase in fracture toughness, while both toughness and stiffness results for the TGDDM-based nanocomposites remained in the same order and appear not to change with the cure temperature.

XRD and TEM work already described has shown that increased cure temperature improved exfoliation, which is often believed to improve mechanical properties. However, it is clear from the neat resin (no clay addition) results in this work that the changes in the initial cure temperature may also affect network forma-

tion and molecular architecture. It can be seen, for example, in Table 3 between 0% organoclay samples that an increase in initial cure temperature increases modulus and toughness (except for toughness data for TGDDM where the toughness is little affected by the higher cure temperature). There are a number of examples for the effect of cure temperature on epoxy network formation alone in the literature: Lewis et al.²⁷ have demonstrated for a DGEBA-based resin system that the thermal history of a fully cured system can significantly affect the glass transition temperature by a variation in T_g of up to 30 °C for resin systems initially cured at different temperatures but all fully postcured. The cure temperature has also been reported to affect etherification and the molecular weight between cross-links,²⁸ M_c . However, changes in the cure schedule appear to affect different epoxy systems in different ways. In their studies on dicyandiamide-cured, benzyldimethylamine catalyzed DGEBA, the group of Sautereau and Pascault et al.^{29–31} found a strong effect of the temperature and accelerator on the reaction mechanism of this system.

Since the organically modified layered silicate in our work has a complex catalytic effect on homopolymerization and resin cure²⁵ with a competition between two or more reactions involving different mechanisms and activation energies, it is likely that the formation of the network structure and therefore thermal and mechanical properties are dependent on the thermal history before postcure. Hence, it is difficult to relate changes in properties of nanocomposites strictly to either issue, i.e., the network structure or the silicate dispersion. Comparison of mechanical properties of the neat resins cured at different temperatures gives an indication how strongly the change in structure in each system is affected by changes in the cure temperature. The neat DGEBA systems cured at 100 and 160 °C show largely improved toughness and stiffness with increased cure temperature, while the two more highly cross-linked resins, TGAP and TGDDM, show only a modest change in modulus.

According to the dramatic changes in the neat DGEBA system with increased cure temperature, it is likely that the enhancement is to a large extent related to variation in the epoxy cure chemistry and hence the polymer matrix, rather than due to a change in delamination of the organoclay platelets within the epoxy phase. This is further confirmed by the fact that the TGDDM-based nanocomposites have shown significantly improved intercalation with increased cure temperature, yet show no major changes in mechanical properties.

The glass transition temperature and degree of unreacted epoxy groups remaining after cure have been investigated using DMTA and FTIR, respectively, to determine other sample differences as a function of cure cycle. The T_g was taken to be the temperature location of the $\tan \delta$ peak at 1 Hz in DMTA measurements. To determine the residual epoxy groups, the area under the 4530 cm^{-1} absorption peak in the FTIR spectra deriving from the epoxy moiety³² was determined and compared with its peak intensity of the unreacted prepolymer blend. Table 4 shows the T_g and percentage residual epoxy groups for neat resins and nanocomposites containing 7.5% organoclay cured at 100 and 160 °C. However, comparison of the T_g as an indicator for the degree of cure can only be applied for the neat systems

Table 4. Comparison of the Glass Transition Temperature (DMTA) and % Residual Epoxy Groups (FTIR) of Neat and Layered Silicate Filled Nanocomposites Cured at 100 and 160 °C

resin system	organoclay [wt %]	T_g [°C]	residual epoxy groups [%]
DGEBA, 100 °C	0	187 ± 1.5	1.2 ± 0.5
DGEBA, 100 °C	7.5	180 ± 1.5	0.1 ± 0.5
DGEBA, 160 °C	0	185 ± 1.5	1.2 ± 0.5
DGEBA, 160 °C	7.5	173 ± 1.5	0.2 ± 0.5
TGAP, 100 °C	0	281 ± 1.5	2.0 ± 0.5
TGAP, 100 °C	7.5	271 ± 1.5	1.6 ± 0.5
TGAP, 160 °C	0	282 ± 1.5	4.0 ± 0.5
TGAP, 160 °C	7.5	269 ± 1.5	1.7 ± 0.5
TGDDM, 100 °C	0	260 ± 1.5	1.4 ± 0.5
TGDDM, 100 °C	7.5	241 ± 1.5	0.8 ± 0.5
TGDDM, 160 °C	0	257 ± 1.5	3.9 ± 0.5
TGDDM, 160 °C	7.5	228 ± 1.5	3.5 ± 0.5

since T_g is likely affected not just by the degree of cure, but also by the presence of clay, with the mechanism being not fully understood. Kornmann et al.,¹⁷ as well as us,⁵ observed a reduced T_g with clay addition and theorized that this may be the result of a number of factors, such as changes in reaction chemistry (epoxy homopolymerization and reduced cross-link density), thermal degradation of the surface modifier, or a plasticizing effect of unreacted resin or hardener monomers. Recent work by Chen et al.³³ has investigated the effect of the cure cycle on the interlayer spacing, the glass transition temperature, and the modulus of an anhydride (hexahydro-4-methylphthalic anhydride)-cured epoxy (3,4-epoxycyclohexylmethyl-3,4-epoxycyclohexane)-layered silicate nanocomposite. The organoclay used was a bis(2-hydroxyethyl)methyl tallow ammonium cation modified montmorillonite. In this work a decrease in T_g and rubbery modulus was seen, and it was proposed to be related to the formation of a lower density interphase consisting of the epoxy resin that is plasticized by the surfactant chains, while the epoxy network formation itself was thought not to be affected by varying the initial cure temperature.

For neat systems it was observed that the higher initial cure temperature has led to a slightly greater level of residual epoxy groups (recalling that all samples are postcured at the same temperature), and this is in good agreement with a slightly decreased glass transition temperature. Organoclay-containing resin systems generally show a higher degree of conversion compared to the neat systems. It can also be observed that these systems further reduce their T_g with increased initial cure temperature and improved exfoliation.

Manipulating the cure temperature may thus lead to both improved exfoliation and modification of the epoxy network. Clearly, variation of the cure profile alone in these systems does not lead to a true, fully exfoliated nanocomposites. Therefore, a combination of both improved cure temperature and processing conditions, including much higher shear forces during cure than used here, or the use of swelling agents,³⁴ which are more effective at entering clay layers than the epoxy monomer, may be the key to the formation of true, individually dispersed epoxy nanocomposites. It should be noted that such homogeneous, individual delaminations have not been demonstrated in any reported TEM images of epoxy nanocomposites yet. Even those systems that were optically clear and deemed exfoliated according to XRD analysis consisted of a blend of partially intercalated and exfoliated silicate layers.¹⁰

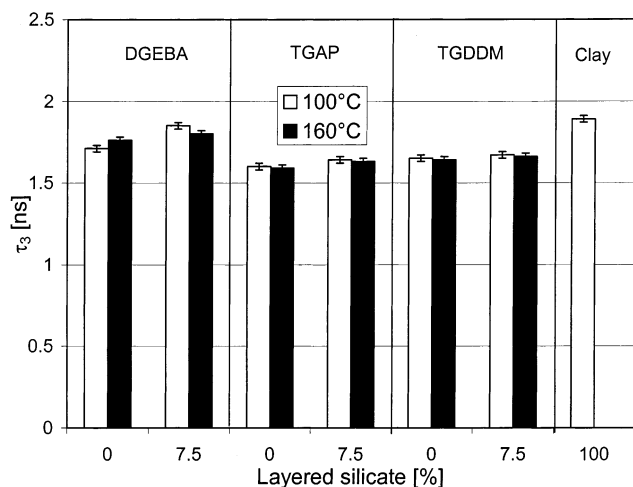


Figure 9. Orthopositronium lifetime, τ_3 (ns), related to the average free volume size of various epoxy and epoxy nanocomposite systems.

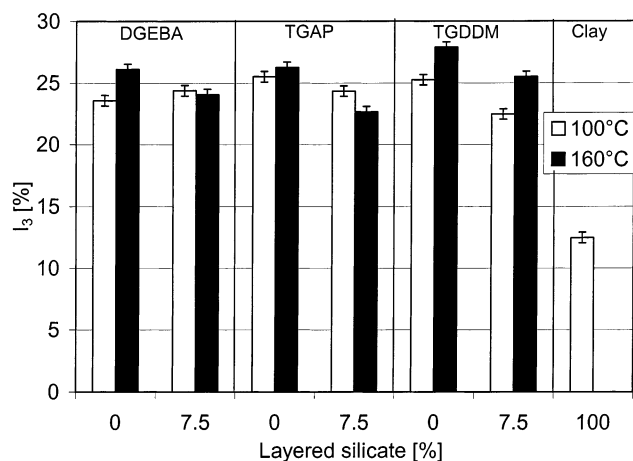


Figure 10. Number concentration of free volume sites (I_3) of various epoxy and epoxy-layered silicate systems.

Free Volume Properties. To date, very little is known about the free volume properties of polymer-layered silicate nanocomposites. The main work reported to date by Olson et al.³⁵ regarding free volume in polystyrene nanocomposites investigated clay-rich composites as a function of temperature, using positron annihilation lifetime spectroscopy (PALS). In brief, it was found that τ_3 of the organically modified layered silicate showed an increase with increasing temperature, plateauing at 90 °C, whereas the I_3 remained relatively constant over the whole temperature range. Both values, τ_3 and I_3 , in the nanocomposite formed by 75 wt % layered silicate and 25% polystyrene were found to be very close to those of the neat silicate, which was reasonable since it was the majority component.

Our work investigates the effect of the organoclay on free volume and molecular packing of unfilled epoxy resins and nanocomposites containing 7.5% organoclay cured at 100 and 160 °C, respectively. Figure 9 is of τ_3 , the orthopositronium lifetime—an indication for the average free volume size, as a function of processing conditions. Figure 10 is of I_3 , a measure of the number concentration of free volume sites of the neat resins and the nanocomposite systems cured at 100 and 160 °C. Only a small difference in the lifetime data of the various resins systems of different structures and functionalities was observed. The τ_3 values were greatest

(and thus highest average free volume size) for DGEBA, followed by TGDDM and TGAP, which had slightly lower values. This variation is likely due to variations in molecular weight between cross-links (low for TGAP) and functionality (high for TGDDM). However, of all the three systems, only the DGEBA τ_3 values are affected by the cure temperature, with a slight increase for higher temperatures. In contrast, the number of free volume sites varied more strongly with cure temperature for all systems, with all I_3 values greater for the neat systems cured at 160 °C. The fact that the average free volume size does generally not change significantly between the two different curing temperatures is in good agreement with the PALS studies on various resin systems (including DGEBA, TGAP, and TGDDM) reported by Jeffery and Pethrick.³⁶ In their free volume studies on chemically different cured resin systems, it was found for a DDS-cured DGEBA that changes in the cure temperature did not lead to significant variation of the mean volume size. In contrast to our work, however, they found that the number of free volume sites was reduced with increasing initial cure temperature, proposed to be related to densification of the resin, consistent with an increased T_g and reduced free volume for higher cure temperatures. In the same work, comparison between DGEBA, TGAP, and TGDDM systems cured with DDM or DDS has shown a significantly lower number of free volume sites for TGAP compared to DGEBA and TGDDM, also not the case in our work. However, the work by Jeffery and Pethrick did show a strong effect of the nature of the chemical structure of the hardener on free volume properties. Hence, it is reasonable that the different structure of the diethyltoluene diamine curing agent used in our work may show different molecular packing than the materials used by Jeffery and Pethrick, in both an absolute and a comparative sense.

Assuming that the free volume sites are of a spherical shape, it is possible to estimate the magnitude of the free volume radius from the semi-empirical equation³⁷

$$\tau_3 = \left[1 - \frac{R}{R_0} + \frac{1}{2\pi} \sin\left(\frac{2\pi R}{R_0}\right) \right]^{-1} \quad (1)$$

with τ_3 being the orthopositronium lifetime (ns), R the radius (Å), and $R_0 = R + \Delta R$ where ΔR is the fitted empirical electron layer and equals 1.66 Å. On the basis of this equation, the free volume diameter in the layered silicate has been calculated as 5.5 Å, to be compared with an average distance of 14.2 Å between the surfaces of the two clay platelets (d spacing minus the layer thickness of 9.6 Å).

Although the PALS free volume radius is of the order of the space between layers, its difference may be due to the fact that the free volume is in layers, rather than spherical holes. It has been found in zeolites and other inorganic molecular solids that the size determined by eq 1, and often more direct methods, is quite close.³⁷ The neat organoclay on its own has a larger average free volume size than the resin systems, and thus according to the rule of mixtures, all materials containing clay may be expected to have larger free volume sizes than the corresponding neat systems, which was found to be the case. By contrast, the DGEBA nanocomposite, particularly that cured at 100 °C, showed a greater value of average free volume size than expected by addition. The number of free volume sites (I_3) of the

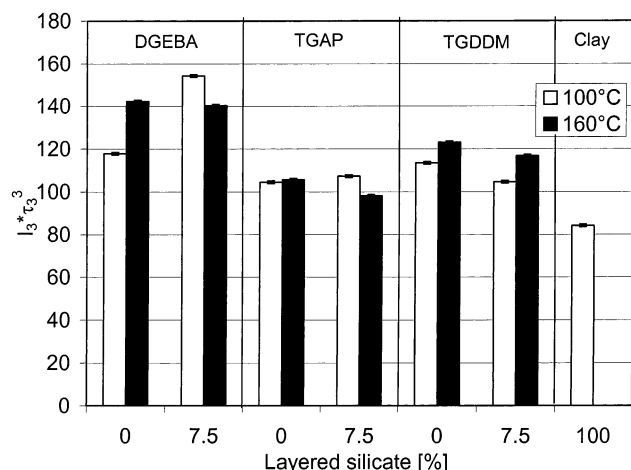


Figure 11. $\tau_3^3 I_3$, indicative of total free volume fraction of various epoxy- and epoxy-layered silicate systems.

organoclay alone is much lower than the values of cured epoxy resins, and most combined epoxy–clay systems showed a concentration slightly above the rule-of-mixture with addition of clay. However, once again in opposition to this trend, the DGEBA nanocomposite cured at 100 °C was the only material that actually showed an increase in free volume site concentration with filler addition. In every other system, I_3 decreases with the filler addition as would be expected from the rule-of-mixtures.

The combination of τ_3 and I_3 behavior combines to yield a synergistically greater total free volume fraction of DGEBA 7.5% at 100 °C, than neat DGEBA, as seen in data for total free volume fraction indicated by $\tau_3^3 I_3$ in Figure 11. This is consistent with the observed lower T_g and reduced degree of cross-link density postulated for epoxy–clay systems by Chen et al.³³ It could be considered that DGEBA would be expected to show most strongly such effects due to the presence of interface and disruption to cross-link density since it contains the best dispersed layers (although, as discussed above, tactoids still exist in conjunction with delaminated layers). However, this is confounded somewhat by the fact that DGEBA at 160 °C, seemingly slightly better dispersed according to TEM, shows the opposite trend—a decrease in total free volume with clay addition. TGAP shows little change at either cure temperature and TGDDM at both cure temperatures shows an increase with clay, as for DGEBA 100 °C. It is thus likely that changes in molecular architecture due to the temperature of cure and degree of exfoliation make simple interpretation of the PALS results difficult. Even considering the difference between neat epoxy and in a binary mixture with clay, the results seem very system dependent, and this may be because, as noted earlier in the DSC results, the catalytic effect of the clay organo-ion on different resins varies significantly. Although all nanocomposites show a lower glass transition with clay addition cured at 100 °C, for example there is differing behavior in total free volume fraction as judged by $\tau_3^3 I_3$, with DGEBA decreasing, TGAP remaining the same, and TGDDM increasing, with addition of clay.

Conclusions

Comparison of the nanocomposite formation based on three different epoxy resins with different structures and functionalities has shown that the structure and

chemistry of the epoxy resin, its mobility and reactivity, are key factors controlling exfoliation and therefore the morphology of the cured nanocomposite. Two different effects have to be considered when the properties of nanocomposites cured at different temperatures are compared: improved dispersion and better exfoliation of the silicate platelets in the polymer matrix as well as changes in the nature of the reaction and thus the network formation. While bifunctional DGEBA resin has shown better exfoliation of the organoclay than the resins of higher functionalities, it was found for all resins that higher cure temperatures led to improved intercalation/exfoliation, although tactoids were observed in all systems including even DGEBA. It seems as though it is the differing effect of the organoclay ion on the reaction of the different epoxies within the galleries that leads to the differences. The structural mobility (diffusion) as indicated by the viscosity of the resin seems less relevant. Relative polarities of the epoxy and modified-clay surfaces—and how they vary as a function of cure—are more difficult to determine and also may have an important impact. It was also clearly demonstrated in the case of DGEBA and TGDDM by kinetic XRD studies that significant intercalation does not simultaneously occur on mixing with resin—but after reaction, still significantly less than gelation. The increased cure temperatures have shown improved modulus and fracture toughness for the DGEBA and (to a lesser degree) for the TGAP nanocomposites. Despite the increased d -spacing in TGDDM nanocomposites, the mechanical properties remained relatively unaffected by the cure temperature. It is assumed that the effect of the cure temperature on the reaction chemistry, i.e., the balance between amine cure and etherification, and the effect on cross-link density also have a major impact on mechanical properties along with the changes in organoclay dispersion. More dramatic changes in the nanocomposite morphology may be required to significantly change the mechanical properties. Since the window of processing temperatures is limited by side reactions and thermal degradation, variation of cure temperature alone may not be sufficient to form a fully dispersed “true” nanocomposite. Free volume measurements showed complex behavior—with some indication of a greater free volume in the systems where the clay is best dispersed—consistent with the lower glass transitions due to reduced cross-link density of interfacial regimes. However, the results are conflicting, even within the same system and for different materials.

Acknowledgment. Jannick Duchet, Henry Sautereau, and Loic Le Pluart of LLM INSA Lyon, France, are acknowledged for their assistance with liquid state XRD measurements and helpful discussions. The Australian Research Council is acknowledged for financial support. Ole Becker also acknowledges the Monash Research Graduate School, the Dr.-Jürgen-Ulstrup Foundation, the German Merit Foundation, and the German Academic Exchange Service (DAAD) for financial support.

References and Notes

- (1) Zilg, C.; Reichert, P.; Dietsche, F.; Engelhardt, T.; Mülhaupt, R. *Kunststoffe* **1998**, *88*, 1812–1820.
- (2) Zanetti, M.; Lomakin, S.; Camino, G. *Macromol. Rapid Commun.* **2000**, *279*, 1–9.
- (3) LeBaron, P. C.; Wang, Z.; Pinnavaia, T. J. *Appl. Clay Sci.* **1999**, *15*, 11–29.

- (4) Alexandre, M.; Dubois, P. *Mater. Sci. Eng.* **2000**, *28*, 1–63.
- (5) Becker, O.; Varley, R. J.; Simon, G. P. *Polymer* **2002**, *43*, 4365–4373.
- (6) Morgan, A. B.; Gilman, J. W.; Jackson, C. L. *Macromolecules* **2001**, *34*, 2735–2738.
- (7) Lan, T.; Kaviratna, P. D.; Pinnavaia, T. J. *Chem. Mater.* **1995**, *7*, 2144–2150.
- (8) Kornmann, X.; Lindberg, H.; Berglund, L. A. *Polymer* **2001**, *42*, 1303–1310.
- (9) Wang, Z.; Pinnavaia, J. T. *Chem. Mater.* **1998**, *10*, 1820–1826.
- (10) Brown, J. M.; Curliss, D.; Vaia, R. A. *Chem. Mater.* **2000**, *12*, 3376–3384.
- (11) Zilg, C.; Thomann, R.; Finter, J.; Mülhaupt, R. *Macromol. Mater. Eng.* **2000**, *280/281*, 41–46.
- (12) Kornmann, X.; Lindberg, H.; Berglund, L. A. *Polymer* **2001**, *42*, 4493–4499.
- (13) Lan, T.; Kaviratna, P. D.; Pinnavaia, T. J. *J. Phys. Chem. Solids* **1996**, *57*, 1005–1010.
- (14) Tolle, T. B.; Anderson, D. P. *Compos. Sci. Technol.* **2002**, *62*, 1033–1041.
- (15) Jiankun, L.; Yucai, K.; Zongneng, Q.; Xiao-Su, Y. *J. Polym. Sci., Part B: Polym. Phys.* **2001**, *39*, 115–120.
- (16) Chin, I.-J.; Thurn-Albrecht, T.; Kim, C.-H.; Russell, T. P.; Wang, J. *Polymer* **2001**, *42*, 5947–5952.
- (17) Kornmann, X.; Thomann, R.; Mülhaupt, R.; Finter, J.; Berglund, L. A. High performance epoxy-layered silicate nanocomposites. In *NRCC/IMI International Symposium on Polymer Nanocomposites Science and Technology, Polymer Nanocomposites*; Montreal, QC, Canada, 2001.
- (18) Xu, W.-B.; Bao, S.-P.; He, P.-S. *J. Appl. Polym. Sci.* **2002**, *84*, 842–849.
- (19) Simon, G. P. *TRIP* **1997**, *5*, 394–400.
- (20) Bigg, D. M. *Polym. Eng. Sci.* **1996**, *36*, 737–743.
- (21) Pethrick, R. A. *Prog. Polym. Sci.* **1997**, *22*, 1–47.
- (22) Puff, W. *Comput. Phys. Commun.* **1983**, *30*, 359.
- (23) JSPDS Powder Diffraction File Database, 1995.
- (24) Ke, Y.; Lü, J.; Yi, X.; Zhao, J.; Qi, Z. *J. Appl. Polym. Sci.* **2000**, *78*, 808–815.
- (25) Becker, O.; Simon, G.; Varley, R.; Halley, P. *Polym. Eng. Sci.*, in press.
- (26) Zilg, C.; Mülhaupt, R.; Finter, J. *Macromol. Chem. Phys.* **1999**, *200*, 661–670.
- (27) Lewis, A. F.; Doyle, M. J.; Gillham, J. K. *Polym. Eng. Sci.* **1979**, *19*, 683–685.
- (28) Varley, R.; Hodgkon, J. H.; Simon, G. P. *J. Appl. Polym. Sci.* **2000**, *77*, 237–248.
- (29) Amdouni, N.; Sautereau, H.; Gérard, J.-F.; Pascault, J.-P. *Polymer* **1990**, *31*, 1245–1253.
- (30) Lin, Y. G.; Sautereau, H.; Pascault, J. P. *J. Polym. Sci. Part A: Polym. Chem.* **1986**, *24*, 2171–2184.
- (31) Lin, Y. G.; Galy, J.; Sautereau, H.; Pascault, J. P. *Crosslinked Polymers*; Sedlacek, B., Ed.; W. de Gruyter: Berlin, 1987; p 148.
- (32) Poisson, N.; Lachenal, G.; Sautereau, H. *Vib. Spectrosc.* **1996**, *12*, 237–247.
- (33) Chen, J.-S.; Poliks, M. D.; Ober, C. K.; Zhang, Y.; Wiesner, U.; Giannelis, E. *Polymer*, in press.
- (34) Salahuddin, N.; Moet, A.; Hiltner, A.; Baer, E. *Eur. Polym. J.* **2002**, *38*, 1477–1482.
- (35) Olson, B. G.; Peng, Z. L.; Srithawatpong, R.; McGervey, J. D.; Ishida, H.; Jamieson, A. M.; Manias, E.; Giannelis, E. P. *Mater. Sci. Forum* **1997**.
- (36) Jeffrey, K.; Pethrick, R. A. *Eur. Polym. J.* **1994**, *30*, 153–158.
- (37) Nakanishi, H.; Wang, S. J.; Jean, Y. C. *Proceedings of International Conference on Positron Annihilation in Fluids*; World Scientific Publishing: Singapore, 1987.

MA0213448